Evolution of the microstructural surface characteristics during annealing

Edgar Gomes[a,*], Kim Verbeken[a], Jai Gautam[b], Leo Kestens[a,b]

[a] *Ghent University, Department of Materials Science and Engineering, Technologiepark 903, B-9052 Gent (Zwijnaarde), Belgium*
[b] *Delft University of Technology, Materials Science and Engineering Department, Mekelweg 2, 2628CD Delft, The Netherlands*

Abstract

In nonoriented electrical steels, the desired cube texture can be obtained at the surface by a double phase transformation annealing. However, the resulting microstructure also displayed several particular features with respect to grain boundaries and in-grain orientation gradients. A careful evaluation of these observations led to a possibly responsible mechanism.

Keywords: EBSD; steel; thermomechanical processing; grain boundaries; orientation relationships; phase transformation

Introduction

During TMP (Thermo Mechanical Processing) of low alloyed steels, the ferrite/austenite/ferrite phase transformation has an impact on the distribution of crystallographic orientations in the material. For these phase transformations, several orientation relationships have been reported to be active; the most commonly cited relationship being the Young-Kurdjumov-Sachs (YKS) relationship where $\{111\}_\gamma \parallel \{011\}_\alpha$, for the closed packed planes, and $\langle 111\rangle_\gamma \parallel \langle 011\rangle_\alpha$, for the closed pack directions. In a crystallographically equivalent representation, this corresponds to 90° rotations about the 24 $\langle 112\rangle$ axes, leading to 24 possible product variants for an arbitrary parent

*Corresponding author
Email addresses: Edgar.Gomes@UGent.be (Edgar Gomes), Kim.Verbeken@ugent.be (Kim Verbeken), jai.gautam@m2i.nl (Jai Gautam), Leo.Kestens@UGent.be (Leo Kestens)

orientation. In case of the double phase transformation the possible number of daughter orientations for each original parent ferrite orientation will be 576 possible equivalent product orientations. The orientation relationships given by YKS are not enough to predict texture evolution during $\alpha \rightarrow \gamma$ and $\gamma \rightarrow \alpha$ transformations since selection mechanisms may operate. Moreover, they may change the texture in different ways, e.g. in $\alpha \rightarrow \gamma$ transformation the texture sharpness is degraded, while during the $\gamma \rightarrow \alpha$ transformation the texture intensity decreased only slightly [1]. But when the double transformation $\alpha \rightarrow \gamma \rightarrow \alpha$ is regarded, one can observe that the final ferrite texture after transformation was inherited from the initial ferrite texture. Such texture memory mechanism was recently reviewed by Hutchinson and Kestens [2].

A $\Sigma 3$ boundary is a low index Coincidence Site Lattice (CSL) boundary between two neighboring grains, of which the misorientation can be described by the $\langle 111 \rangle 60^\circ$ axis/angle pair. This type of boundary can be either 'coherent', when it is accompanied by a $\{111\}$ grain boundary plane, either 'incoherent' for all other planes. Incoherent $\Sigma 3$'s with tilt or twist planes have higher free volumes than $\Sigma 3$ coherent twins on $\{111\}$ planes, nevertheless they exhibit still a much lower than average grain boundary energy value when compared to a random high angle grain boundary. The properties of coherent and incoherent $\Sigma 3$ boundaries may differ in many aspects, such as for example their mobility. Coherent $\Sigma 3$ boundaries are practically immobile while incoherent $\Sigma 3$ boundaries are very mobile. Despite the differences between the types of boundaries in the $\Sigma 3$ group, it can be said that potentially all $\Sigma 3$'s have properties that are different from random boundaries [3]. In addition to all factors that govern the microstructural changes during annealing in the bulk of a material, additional effects play a role at the material surface. Of considerable influence at the sample surface during phase transformations are additional forces that originate from the metal/vapour interface. Hashimoto et al. [4, 5] investigated the $\alpha \rightarrow \gamma \rightarrow \alpha$ phase transformation texture at the surface of an ultra low carbon cold rolled steel sheet and reported that a $\langle 100 \rangle \parallel ND$ texture was formed rather than the usual $\langle 111 \rangle \parallel ND$ texture. Aspden et al. [6] reported that an annealing treatment for an ultra low carbon steel in the austenitic temperature region followed by a slow cooling resulted in a stronger $\langle 100 \rangle \parallel ND$ texture. In all of these works it was assumed that the resulting surface texture was produced due to the lowest metal/vapour interface energy in the $\{001\}$ fibre. In the literature only textural changes are discussed, excluding a precise description of the grain

C $[wt\%]$	Mn $[wt\%]$	Si $[wt\%]$	Al $[wt\%]$
0.002	1.28	0.22	0.29

Table 1: Chemical composition.

morphology and grain structure at the surface. Therefore, in this work, apart from the crystallographic texture, the grain morphology and grain boundary characteristics at the sample surface will be further explored.

Experimental procedure

The material under consideration is an ultra low carbon (ULC) steel with additions of manganese and aluminium as summarized in Table 1.

After hot rolling, air cooling and annealing at $700°C$ were applied to simulate the slow cooling in an industrial production line. After acid pickling, the hot rolled sheet was cold rolled to a final thickness of $0.5mm$ by a reduction of 70%. Subsequently, an annealing cycle was performed to induce the formation of cube texture at the surface by $\alpha \rightarrow \gamma \rightarrow \alpha$ transformation in a controlled reducing atmosphere of a $5\%\, H_2 - 95\%\, N_2$ mixture at $1050°C$. The cold rolled sheets were heated with a rate of $15°C/s$, held at $1050°C$ for $120s$ and cooled at $30°C/s$ to room temperature. An XL-30 SEM (FEI) equipped with Electron Backscatter Diffraction (EBSD) was used to measure the microstructural details and orientation imaging microscopy both at the surface and in the bulk of the sample.

Results

The crystallographic texture was analyzed at different ND sections in order to evaluate texture changes across the sample thickness. This revealed that after annealing, the typical cold rolling and annealing ND fibre texture was present in the bulk of the material, see Figure 1 (a). As expected a different crystallographic texture was revealed at the sample surface: the annealing treatment led to the formation of recrystallized grains with a relatively weak intensity on the cube ($\langle 001 \rangle \parallel \overrightarrow{ND}$) texture and an even weaker intensity of $\langle 110 \rangle \parallel \overrightarrow{ND}$ orientations, see Figure 1 (b). It was found by considering various ND-sections of the material that the surface texture resulted from a thin layer of recrystallized grains formed from surface to about $30\mu m$ deep into the sample, further informations are given elsewhere [7, 8].

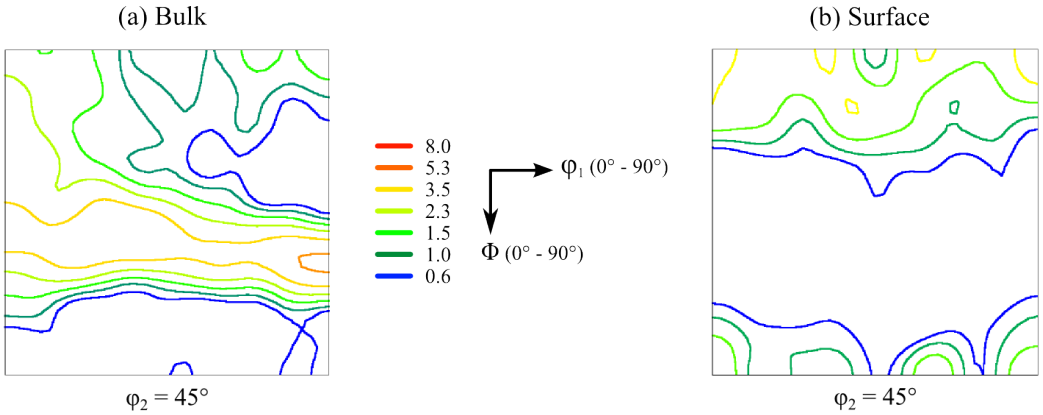

Figure 1: Orientation distribution function (ODF) at the $\varphi_2 = 45°$ section for both bulk (max = 5.8) and surface (max = 2.9) of the material. Levels: $(0.6 - 1.0 - 1.5 - 2.3 - 3.5 - 5.3 - 8.0)$.

Even though the surface texture was not really surprising; the other microstructural characteristics at the surface were quite remarkable. The cube fibre grains exhibited in-grain orientation gradients with a gradual orientation shift occurring smoothly and with linear profile. This gradual shift was observed after the annealing treatment and only for these specific orientations and at the sample surface. As is shown on Figure 2, the typical value for the shifting rate ranged between 0.12 and $0.16°/\mu m$. In the same figure, it is shown that these grains, besides the orientation shift also have an 'X' like morphology, where in the centre $\{001\}$ orientations are present and the 'arms' display a texture gradient shifting away from $\{001\}$ rotating smoothly about a $\langle 100 \rangle$ axis towards the edge of the grain, more details on this observation are given elsewhere [9]. When going into more detail for the analysis of surface microstructure, Figure 3 revealed that the grain boundaries at the surface had a rather irregular shape in comparison with the flat faced grains in the bulk of the material. Moreover, when considering the specific grain boundary, $\Sigma 3$ CSL interfaces were found on the surface layer with an increased fraction of at least two times more than the middle section, shown in Table 2. Island grains, most of them surrounded by $\Sigma 3$ boundaries, can be observed in the surface microstructure, see Figure 3. Frequently such island grains are considered to be the result of a stalled growth process. The $\Sigma 3$ boundaries are generally associated with a decreased mobility, this also may be the case here.

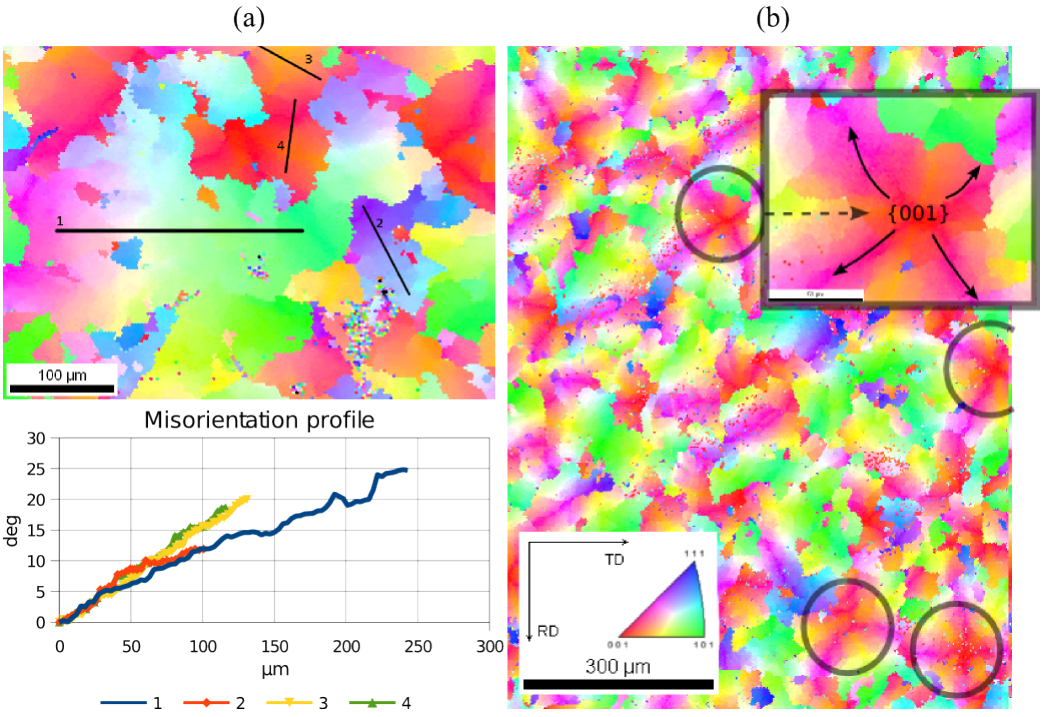

Figure 2: (a) - IPF map of ND section showing the in-grain texture gradients and the lines of measurement. The graphic below displays the misorientation profile of the respective lines. (b) - IPF (Inverse Pole Figure) map of the ND section showing the 'X' like grain morphology. An image at higher magnification shows the 'arms' going towards the grain boundary.

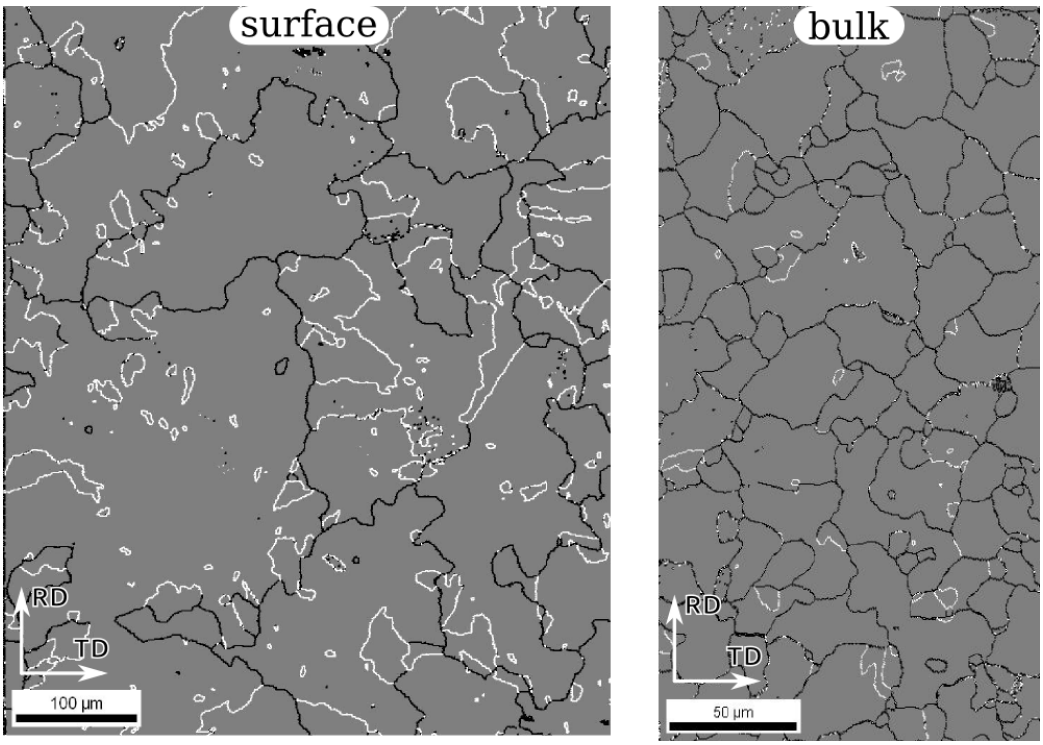

Figure 3: Grain boundary partition at surface. High angle grain boundaries and $\Sigma 3$ interfaces are represented in black and white lines, respectively.

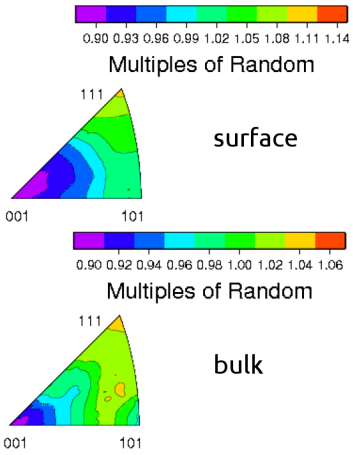

Figure 4: Grain boundary character distribution for all misorientations.

	Surface	Bulk
$\Sigma 3$	40.5%	10.3%
Coherent $\Sigma 3$	0.89%	0.90%

Table 2: Fractions of $\Sigma 3$ CSL boundaries.

A grain boundary requires of course 5 parameters to be described completely. Apart from the 3 parameters that describe the misorientation, two other parameters are needed to describe the grain boundary plane inclination. Since these two parameters cannot be obtained from a two dimensional measurement, an approximation obtained by applying the method developed by Rohrer et al. [10] was performed. This software can estimate the GBCD (Grain Boundary Character Distribution) in a statistic manner based on two dimensional reconstructed grain boundary line segments gathered from a EBSD measurement. It is important to note that, in the present case, the recommended range of input data for this software was not achieved, as it requires at least $50,000$ segments for typical cubic symmetry situations. Another prerequisite is that the Misorientation Distribution Function (MDF) should not have any significant texture, since this will cause the results to be accurate at the misorientations that are highly populated, but inaccurate at those that are not. Therefore, the present results should be considered as giving a tendency rather than exact values. The plane direction distribution of GBs of all misorientations displays a relatively low intensity of $\langle 001 \rangle$ GB poles and a high intensity of $\langle 111 \rangle$ GB poles in both surface and central sections, see Figure 4. For the specific case of $\Sigma 3$ CSL boundaries, it was found that only a fraction as low as 2% of all $\Sigma 3$ interfaces were coherent in both surface layer and bulk region, see Table 2. This result is in agreement with the $\Sigma 3$ boundary shape, as it shows a complete absence of flatness. In order

to get a better grip on the observed structures, simulations were carried out with respect to the texture evolution caused by the $\alpha \rightarrow \gamma \rightarrow \alpha$ phase transformation. A perfect ND fibre was used as initial texture for the calculations which consisted in rotations according to the YKS orientation relationship. The first transformation ($\alpha \rightarrow \gamma$) gave rise to 24 products orientations for each component of the initial gamma fibre. A second transformation ($\gamma \rightarrow \alpha$) was applied on the result of the first one. For both transformations, no variant selection mechanism was applied. These calculations showed a weak and widely spread texture with some intensity concentration on the ND fibre and even weaker intensity on the cube fibre.

Discussion

A texture evolution simulation of the $\alpha \rightarrow \gamma \rightarrow \alpha$ transformation, assuming YKS orientation relations, exhibits a weak texture which includes the $\{111\}$ fibre but also some $\{001\}$ fibre components. When this result is compared to the texture observations at the bulk and at the surface of the sample, it can be argued that the texture components with the highest intensity both at the surface and in the bulk were present in this simulation. With respect to the bulk, a stronger $\{111\}$ fibre texture and limited intensities for other components were observed. This could, however, be expected taking into account the texture memory mechanism, as recently reviewed by Hutchinson and Kestens [2]. At the surface, the presence of $\{001\}$ was predicted, but the presence of $\{110\}$ fibre orientations and also the complete absence of $\{111\}$ fibre orientations reveals the possible existence of another orientation selection mechanism operating at the surface. Such mechanism has favoured $\{001\}$ and $\{110\}$ nucleation. It seems quite reasonable to assume that the crystal anisotropy of surface energy at the metal/vapour interface is responsible for this orientation selection. As the $\{001\}$ fibre orientations are already present among expected transformation product orientations, it seems logic that these orientations have a higher intensity than $\{110\}$ fibre orientations.

With the gradual evolution of the $\alpha \rightarrow \gamma \rightarrow \alpha$ transformation, it appears that the $\{001\}$ grains underwent a crystal lattice rotation during growth that can be accommodated either plastically (by dislocation walls of low angle grain boundaries) or either elastically. A distinction between both cannot be made based on the present data. The in-grain orientation shift, with the grain starting from a $\{001\}$ nucleus and rotating away from this

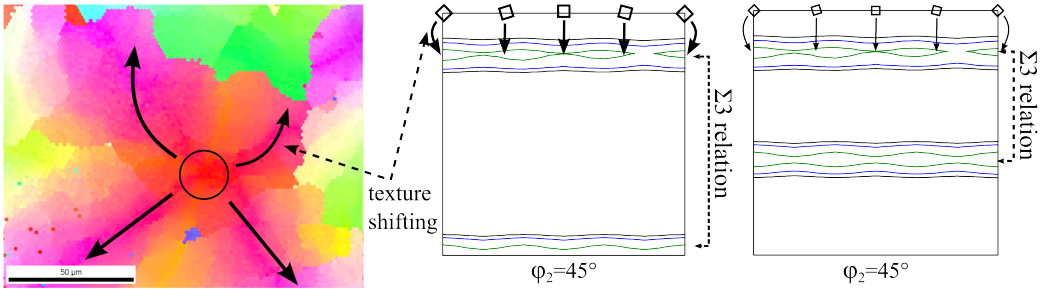

Figure 5: Schematic illustration of the proposed mechanism. Cube surface grains rotate downwards ($\Phi = 15°$) to match {115} fibre which exhibits a $\Sigma 3$ relation with both {110} orientations at the sample surface and {111} orientations in the bulk of the material.

starting orientation, requires a different explanation. It seems that another orientation selection mechanism is responsible for this. It may be reasonable to assume that in the underlying layer (of non-surface grains), dominated by {111} orientations due a texture memory effect, gradually not only the metal/vapour surface energy is of importance but also the metal/metal grain boundary energy starts having an influence. Therefore, as the anisotropy of surface energy in the metal/vapour interface led to a {001} selection, the anisotropy of the surface energy at the metal/metal interface enhances the formation of low energy $\Sigma 3$ boundaries. This can be reached by a gradual rotation of the {001} nucleus to a near cube fibre orientation, that forms a $\Sigma 3$ interface with the {111} fibre orientations of the underlying layer. As the in-grain rotation observed at the outer rim of the surface grains [9] is $\Phi = 15°$, which is precisely the orientations that have a $\Sigma 3$ ($\langle 111 \rangle\, 60°$) interface with the bulk texture, composed of {111} fibre grains. Moreover, this very same in-grain rotation of the {001} nucleus also gives rise to a low energy $\Sigma 3$ boundary with the {110} fibre grains that are also present in a more than random quantity at the sample surface. The suggested mechanism for the observed in-grain rotation is schematically illustrated in Figure 5 and might provide an explanation for two observed features in the sample, namely the in-grain rotation of surface grains and the increased incidence of $\Sigma 3$ boundaries at the surface.

Conclusions

This paper describes the appearance of an intriguing surface microstructure evolved during the $\alpha \rightarrow \gamma \rightarrow \alpha$ annealing of a cold rolled sample of an ULC steel. An explanation for the observed phenomena is proposed. While the texture and grain morphology in the bulk could be attributed to the YKS relationship in addition to a memory effect, at the metal surface also the surface energy anisotropy plays a dominant role, giving rise to a surface $\{001\}$ and $\{110\}$ fibre texture. Besides the appearance of this texture, a specific surface microstructure has developed with irregular grain boundary shape, a high frequency of $\Sigma 3$ boundaries and strong in-grain orientations gradients. It appears that the ensuing texture and microstructure are the result of a process in which the overall interface energy is minimized, pertaining both to the metal/vapor interface and the metal/metal grain boundary interface.

References

[1] G. Brückner, J. Pospiech, I. Seidl, G. Gottstein, Orientation correlation during diffusional $\alpha \rightarrow \gamma$ phase transformation in a ferritic low carbon steel, Scripta Materialia 44 (11) (2001) 2635–2640.

[2] B. Hutchinson, L. A. I. Kestens, Origins of texture memory in steels, in: Applications of Texture Analysis, vol. 201 of *Ceramic Transactions*, 281–290, 15th International Conference on Textures of Materials, Pittsburgh, PA, Jun 01-06, 2008, 2009.

[3] V. Randle, Twinning-related grain boundary engineering, Acta Materialia 52 (14) (2004) 4067–4081.

[4] O. Hashimoto, S. Satoh, T. Tanaka, Effects of Initial Texture on $\alpha \rightarrow \gamma \rightarrow \alpha$ Transformation Texture in Sheet Steel, Tetsu-to-hagane 66 (1980) 112.

[5] O. Hashimoto, S. Satoh, T. Tanaka, Formation of $\alpha \rightarrow \gamma \rightarrow \alpha$ Transformation Texture in Sheet Steel, Tetsu-to-hagane 66 (1) (1980) 102–111.

[6] R. Aspden, J. Berger, H. Trout, Anisotropic and heterogeneous nucleation during the gamma to alpha transformation in iron, Acta Metallurgica 16 (8) (1968) 1027–1035.

[7] J. Gautam, R. Petrov, L. Kestens, Surface texture evolution during α–γ–α transformation in Mn and Al alloyed ultra-low carbon steel, in: Materials science forum, vol. 550, Trans Tech Publ, 503–508, 2007.

[8] J. Gautam, R. Petrov, L. Kestens, E. Leunis, Surface energy controlled α–γ–α transformation texture and microstructure character study in ULC steels alloyed with Mn and Al, Journal of Materials Science 43 (11) (2008) 3969–3975.

[9] J. Gautam, Control of Surface Graded Transformation Texture in Steels, Ph.D. thesis, Delft University of Technology, NL, 2011.

[10] G. Rohrer, D. Saylor, B. El Dasher, B. Adams, A. Rollett, P. Wynblatt, The distribution of internal interfaces in polycrystals, Zeitschrift fur Metallkunde 95 (4) (2004) 197–214.